

Statistical Analysis of Factors Affecting the Dry Sliding Wear Behaviour of Al/SiC_p on Automobile Friction Material

¹R.H.Naravade, ²R.K.Belkar

¹Lecturer, Department of Mechanical Engineering, P.Dr.V.V.P.Polytechnic, Loni

²Head of Department, Department of Mechanical Engineering, P.Dr.V.V.P.Polytechnic, Loni

ABSTRACT

This study covers statistical analysis of the major tribological factors affecting the dry sliding wear behaviour of Al-SiC_p-brake pad system. The composite material for investigation was developed by stir casting technique from Al 6082 alloy by incorporating 15% SiC_p by weight. The factors selected for investigation were temperature, load and sliding velocity keeping sliding distance constant. The wear test was done on Pin on Disk wear testing machine. Commercially available brake pads were used as the pin material. Hardness survey, Optical microscopy and SEM were used to characterise the materials before and after the wear tests. Worn surfaces and debris were characterised using SEM to understand the wear mechanisms. ANOVA results show that temperature is the most dominant factor affecting the wear rate.

Date of Submission: 14 November 2014



Date of Accepted: 05 December 2014

I. INTRODUCTION

Aluminium Matrix Composites (AMCs) are finding extensive applications in the aerospace and automotive industries because of their superior mechanical and tribological properties. The increasing demand for lighter weight and fuel efficient materials is leading the contemporary research to the development of more advanced MMC materials [1]. The particle reinforced AMCs offer a better candidature as an advanced material due to its enhanced properties. The improved properties are high specific heat capacity and thermal conductivity among thermal properties and low density, high specific strength, high specific stiffness, controlled coefficient of expansion, fatigue resistance and superior dimensional stability among physical properties [2]. AMCs with excellent properties are tailor made with different manufacturing methods like powder metallurgy, liquid metal infiltration, squeeze casting, etc. [3–6]. Generally used particulate reinforcements include SiC, Al₂O₃, etc. Wear resistance of AMCs was found to be increasing with increase in percentage addition of reinforcement [7–9]. Different mechanisms operating in the wear of AMC are found to be oxidation, delamination, adhesion and thermally activated severe wear [10]. Wear mechanisms are understood by conducting characterisation studies of wear surface and debris particles using XRD, SEM, EDX, etc. [11–14].

The study of tribological behaviour of AMCs with brake pads is very important as it can help to improve the efficiency of braking and hence can design better braking systems. So, wear studies of AMC-brake pad tribosystem have fetched a lot of attention in recent times [15–17]. Commercial brake pads are classified as organic, metallic and semi metallic depending on its constituents [18–20]. The study on the sliding wear behaviour of A356/25SiC_p against automobile friction revealed the wear of AMC is lower than cast iron and it has higher and stable friction coefficient than cast iron [21]. Therefore AMC can be regarded as a better candidate for brake applications. Understanding of the tribofactors is important to study the behaviour of AMC-brake pad system. The statistical analysis of factors influencing the wear of this system is thus very significant in designing the brake discs of an automobile. Though literature is available on statistical studies of AMCs with other mating materials [22–24]. Studies were done before and after wear test employing optical microscopy (OM), hardness survey and scanning electron microscopy (SEM).

II. EXPERIMENTAL WORK

Aluminium metal matrix composite was produced by liquid casting route using conventional casting methods. Al6082 alloy was melted at 750 °C and preheated SiC particles (15% by weight) were added to the

molten aluminium alloy. The SiC particles were mixed in the semisolid stage to obtain a uniform distribution of the reinforced particles. The average SiC particle size ranges from 30 to 70 μm . The as-cast cylindrical composite was machined and made into cylindrical discs of 48 mm diameter and 10 mm thickness. The hardness of the composite was found to be Hv_1 55. The discs were polished with 1000 grit emery paper to have roughness values ranging from Ra 0.50 to 1.1 μm .

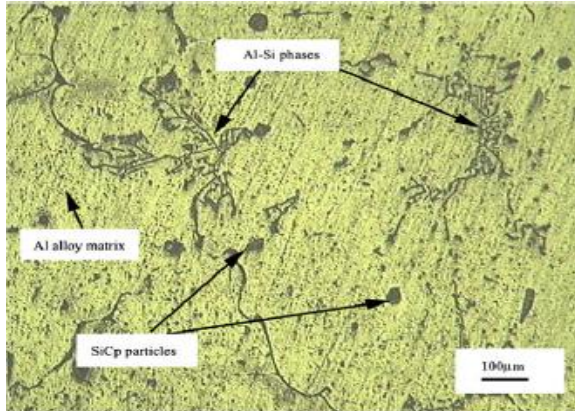


Fig. 1. Microstructure of Al-SiCp composite showing distribution of SiCp.

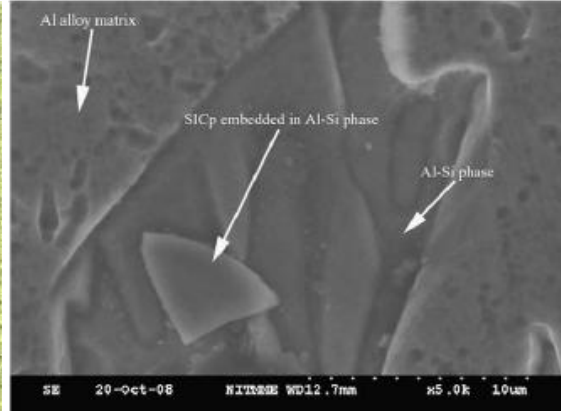


Fig. 2. SEM micrograph of AMC showing SiC in Al-Si phase.

Figs. 1 and 2 show the distribution of SiC particles in the aluminium matrix and their morphology, respectively. Pins were made from commercially available brake pads for light weight passenger vehicles. These semi metallic brake pads were machined in the form of rectangular pins. The dimensions of the pins are $7 \times 7 \times 30 \text{ mm}^3$. The pins were ground using belt grinding and the roughness values were found to be in the range of Ra 1 to 1.5 μm .

A. Experimental Procedure

The dry sliding tests were carried out using a high-temperature pin-on-disc equipment. The pin and disc were cleaned using ultrasonic cleaning with acetone and weighed before and after each experiment using a weighing balance of accuracy 0.1 mg. Plan of experiments was made by Central Composite Design selecting the face centered points. The levels selected for each factor in the design are shown in Table 1. The Design Expert 7 software was used for designing the experiments. The plan of experiments was made by randomising the experiments to avoid accumulation of errors. The experiments were conducted based on the randomised run number as mentioned in Table 2. Wear rate of the composite was taken as the response.

Table 1 Factors and their levels chosen for face centered Central Composite Design.

Level	Temperature ($^{\circ}\text{C}$)	Load (N)	Sliding velocity (m/s)
-1	25	10	0.5
0	100	15	1
+1	175	20	1.5

Table 2 Plan of experiments.

Std	Run	Factor 1 A: temperature ($^{\circ}\text{C}$)	Factor 2 B: load (N)	Factor 3 C: velocity (m/s)
11	1	100	10	1
4	2	175	20	0.5
15	3	100	15	1
12	4	100	20	1
20	5	100	15	1
6	6	175	10	1.5
19	7	100	15	1
2	8	175	10	0.5
18	9	100	15	1
10	10	175	15	1
17	11	100	15	1
16	12	100	15	1
8	13	175	20	1.5
1	14	25	10	0.5
5	15	25	10	1.5
3	16	25	20	0.5
7	17	25	20	1.5
13	18	100	15	0.5
14	19	100	15	1.5
9	20	25	15	1

The experiment consisted mainly of three phases. Initially a run in wear test was conducted for making the pin flat, and then it was run with the AMC specimen disc for about 10 min to avoid initial vibration of friction. In the third stage the experiment was conducted at the real wear testing conditions. For high temperature experiments the furnace was heated to the required temperature and was allowed to stabilise for 1 h. Constant sliding distance of 1.5 km was maintained for all the experiments. The wear debris was collected during the experiments. The frictional force was directly read using LabVIEW software. Mass loss of pin and disc, width

of wear track and average diameter of wear track was noted down after each experiment. Coefficient of friction was found out by dividing the average of the frictional force during the experiment with the normal load applied. The wear rate was calculated by dividing the mass loss of the disc with the total area of sliding undergone by the disc. The wear surface and debris were examined using OM and SEM. Cross sections of the wear tracks across the sliding direction were taken for SEM analysis and hardness survey.

III. RESULTS AND DISCUSSION

A. ANOVA of wear rate

The analysis of the wear rates obtained from the experiments (Table 3) was done using statistical analysis software Design Expert 7.

Table 3
Results of experiments.

Std	Run	Factor 1 A: temperature (°C)	Factor 2 B: load (N)	Factor 3 C: velocity (m/s)	Response 1 Wear rate (g/mm ² × 10 ⁻⁷)
11	1	100	10	1	2.0998
4	2	175	20	0.5	12.3048
15	3	100	15	1	8.9371
12	4	100	20	1	17.9483
20	5	100	15	1	18.2400
6	6	175	10	1.5	15.2156
19	7	100	15	1	6.9747
2	8	175	10	0.5	8.8926
18	9	100	15	1	17.1834
10	10	175	15	1	15.6508
17	11	100	15	1	18.8052
16	12	100	15	1	14.8293
8	13	175	20	1.5	31.3914
1	14	25	10	0.5	0.9851
5	15	25	10	1.5	1.9779
3	16	25	20	0.5	18.0670
7	17	25	20	1.5	0.4714
13	18	100	15	0.5	3.0356
14	19	100	15	1.5	15.4480
9	20	25	15	1	7.9188

Fig. 3 shows the standard error of the design which is found to be uniform and thus favourable. A regression model is generated by fitting the experimental data with the help of the software. The cubic model is aliased, so reduced quadratic model is used for fitting the data.

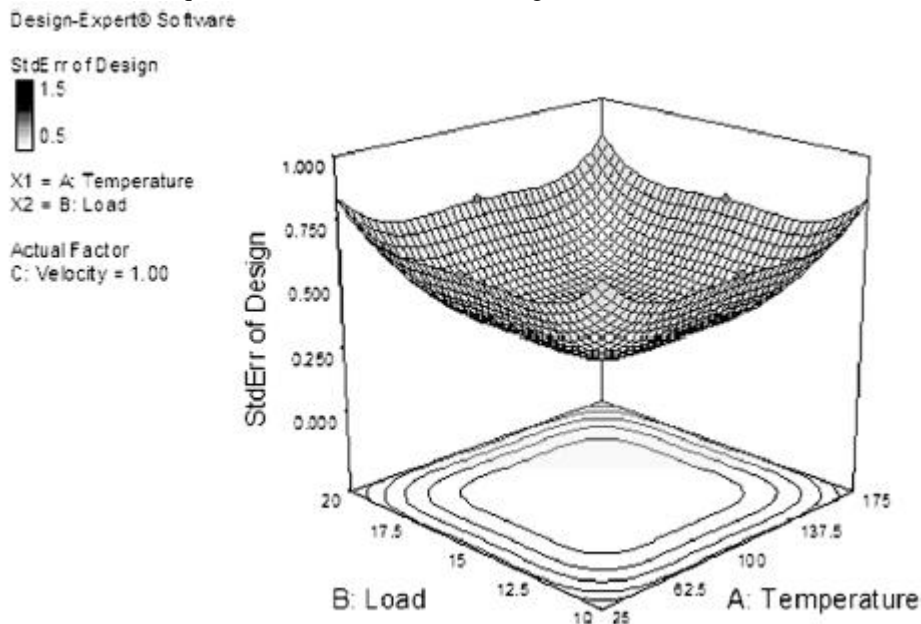


Fig. 3. Variation of standard error in the design space.

The model is coded using letters A, B and C. A corresponds to temperature, B to load and C to sliding velocity. The quadratic model is reduced by removing the model terms A2, B2 and C2 to make the model significant. The ANOVA results are as shown in the Table 4.

Table 4
ANOVA results for reduced quadratic model.

Response 1		Wear rate				
ANOVA for response surface 2FI model						
Analysis of variance table [Partial sum of squares - Type III]						
Source	Sum of squares	df	Mean square	F Value	p-Value Prob > F	
Model	824.106647	6	137.35111	4.78416435	0.0087	Significant
A - temperature	291.977578	1	291.97758	10.1700579	0.0071	
B - load	260.22094	1	260.22094	9.06392211	0.01	
C - velocity	45.0252987	1	45.025299	1.568305	0.2325	
AB	2.01265548	1	2.0126555	0.07010409	0.7953	
AC	220.629147	1	220.62915	7.68487503	0.0159	
BC	4.24102908	1	4.2410291	0.147722	0.7069	
Residual	373.223884	13	28.70953			
Lack of fit	246.503245	8	30.812906	1.21578087	0.4333	Not significant
Pure error	126.720639	5	25.344128			
Cor total	1197.33053	19				

Temperature (A), load (B) and temperature– velocity interaction (AC) are found to be the significant factors. Values of “Prob > F” less than 0.0500 indicate model terms are significant. F values greater than 0.1000 indicate that model terms are not significant. The results show that velocity (C), temperature– load interaction (AB) and load–velocity interaction (BC) are insignificant. The “Lack of Fit F-value” of 1.22 implies that lack of fit is not significant relative to the pure error. There is a 43.33% chance that a “Lack of Fit F-value” this large could occur due to noise. Non-significant lack of fit is good for the model to be fit. The most significant factor that affects the wear rate response is the temperature as it shows the least p-value. The Final regression equation in terms of actual terms is indicated below:

$$\begin{aligned} \text{Wear rate} = & - 3.29139 - 0.088058 * \text{Temperature} + 1.17772 \\ & * \text{Load} - 5.39167 * \text{Velocity} + 1.33755E - 003 \\ & * \text{Temperature} * \text{Load} + 0.14004 * \text{Temperature} \\ & * \text{Velocity} - 0.29124 * \text{Load} * \text{Velocity} \end{aligned}$$

Diagnostics were done and satisfactory results for normal plot of residuals were obtained. From Box-Cox plot for power transforms, Lambda value of nearly one suggests that no transformation is recommended for the wear rate analysis. Fig. 4 shows the 3D response surface graphs of wear rate against load and temperature at three different levels of velocity.

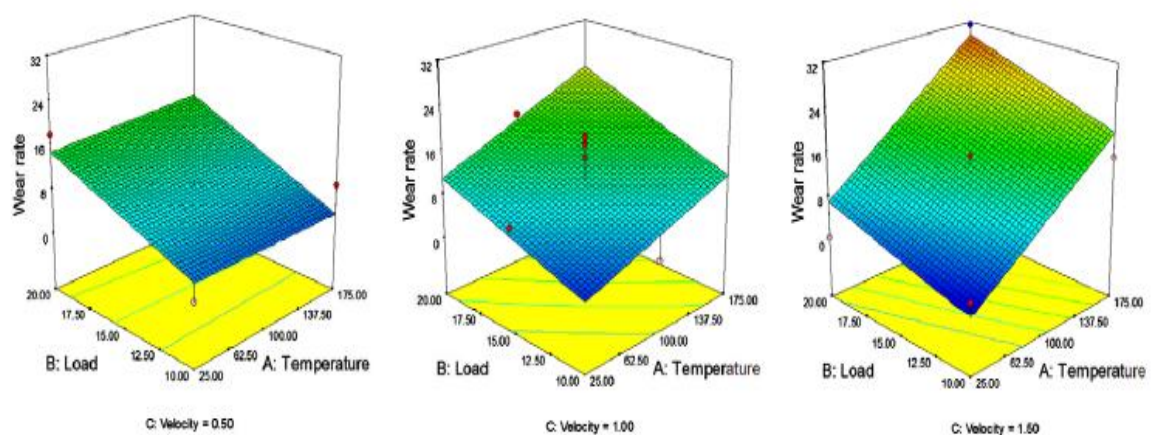


Fig. 4. 3D response surface at three different velocity levels.

B. Wear Analysis

Figs. 5 and 6 show the surface morphology of wear tracks at two different experimental conditions. It can be observed that at low temperatures and loads the surface profile is shallow as compared to the wear tracks at high temperature and loads. The AMC surface had undergone mild wear which can be attributed to the oxidative wear mechanism. Oxide layers were formed on the surface of the composite as the pin scratches away

some of the surface material. This oxide layer restricts further removal of material by restricting the formation of transfer layer [26]. At room temperature and moderately high temperatures mild wear is observed where oxidative mechanism is the dominating over adhesive wear mechanism.

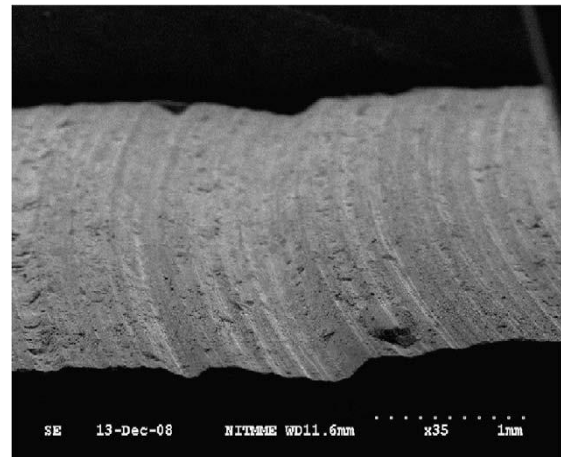
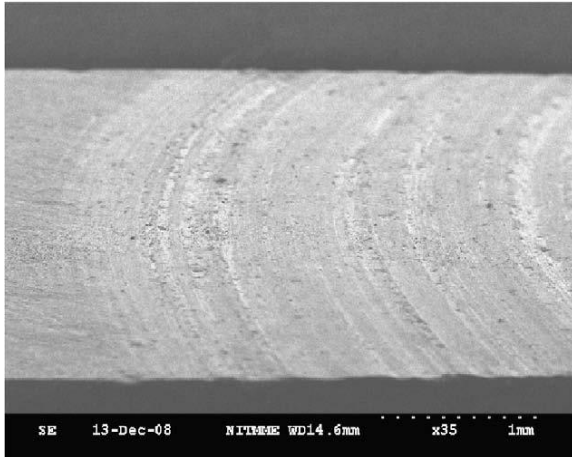


Fig. 5. Surface morphology of wear track after mild wear.

Fig. 6. Surface morphology of wear track after severe wear.

At high loads and temperatures the composite showed severe wear (Fig. 6). This can be attributed to the heavy removal of matrix material by hard transfer particles. Under these conditions the SiCp loses its ability to carry the load and it gets fractured adding to the wear debris. This leads to cracking of the aluminium matrix followed

by delamination (Fig. 7). At high temperature, the formation of transfer layer due to adhesion is found to be faster and in turn produces the transfer particles. These strain hardened transfer particles removes oxide layer and the mating surfaces come directly in contact with each other. The transfer particles are harder than the substrate material. These hard transfer particles form deep grooves on the surface of the disc. Deep groove formations in the wear tracks are characteristic of an adhesion induced-tribofracture mechanism. Fig. 7 shows the ploughing and groove formation due to the transfer particle. At high velocities, this transfer mechanism was

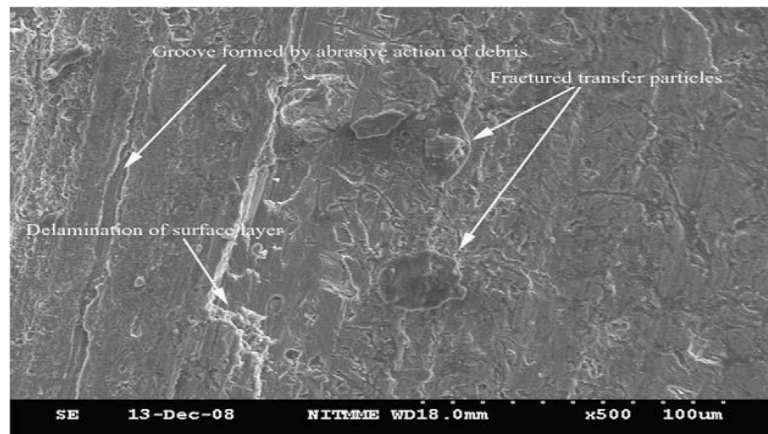


Fig. 7. SEM micrograph of a worn surface after sever wear.

so quick that more and more transfer particles are formed and removed from the surface of the disc. The rate of wear of the transfer particle is equal to the wear rate of the disc [26]. Thus it can be learnt that at high levels of tribofactors oxidative wear mechanism is completely superceded by the quick adhesive wear mechanism. At moderate levels of temperature and loads the wear is due to these two competing mechanism. At moderate loads SiCp in the AMC carries the load and reduces the delamination of aluminium matrix. The pullout of SiCp particles from the matrix reduced the hardness of the surface layer. But the subsurface layer as hardened due to the action of transfer particles. This is confirmed by the microhardness survey using Vicker's hardness as shown in Fig. 8.

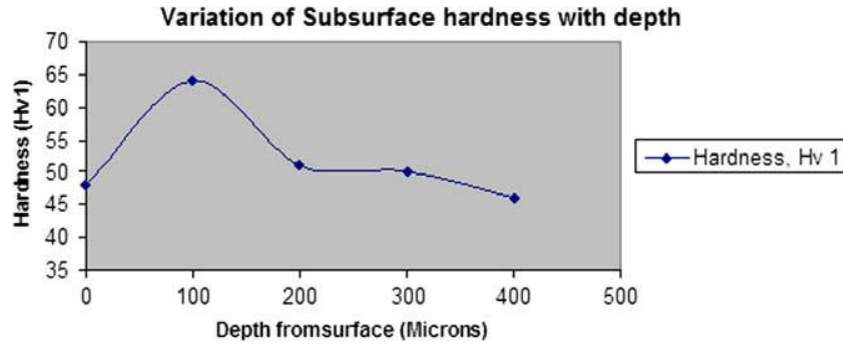


Fig. 8. Variation of hardness across the depth of AMC after wear.

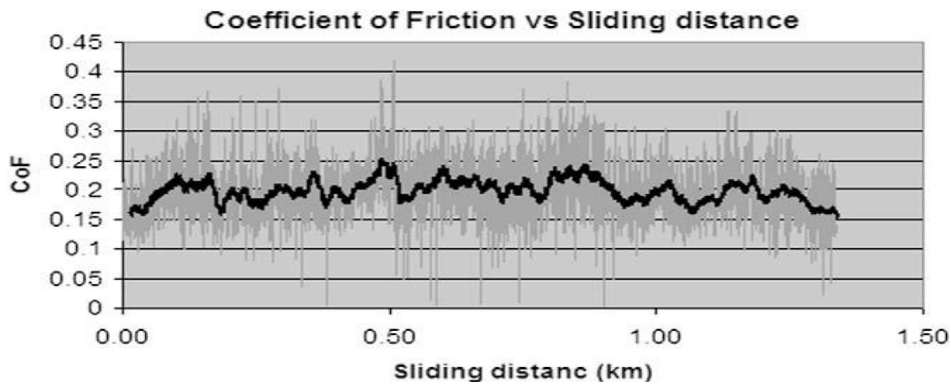


Fig. 9. Variation of coefficient of friction with sliding distance.

The frictional coefficient through out the experiments was almost constant which is very favourable for the use of this system in braking systems. Fig. 9 shows the variation of coefficient of friction vs sliding distance for a typical experiment at 100 °C. The value of CoF was found to be varying from 0.2 to 0.5 for most of the conditions which is suitable for the braking applications.

C. Effects of Temperature

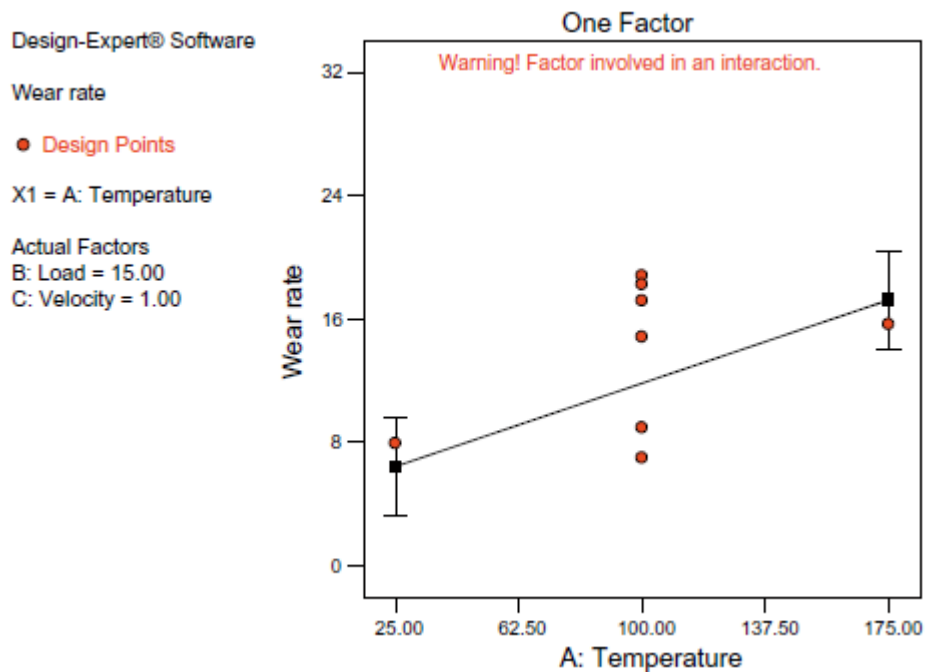


Fig. 10. Variation of wear rate with temperature.

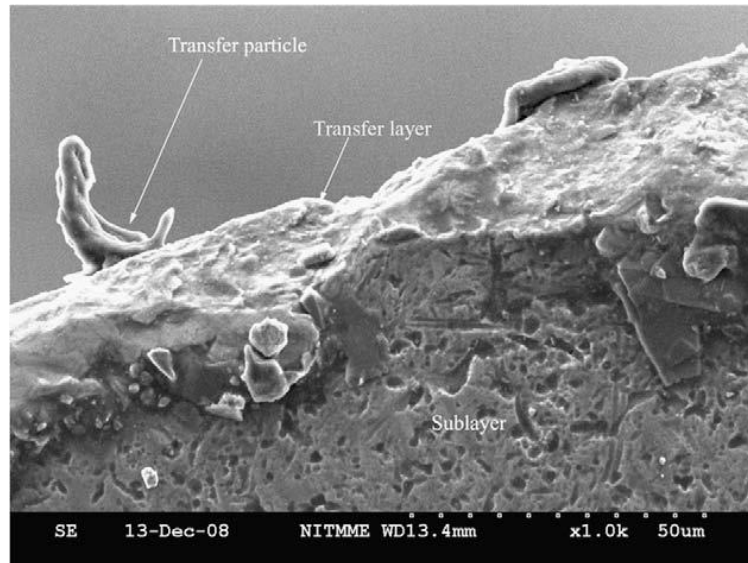


Fig. 11. SEM micrograph of transfer layer.

Fig. 10 shows the effect of temperature on the wear rate. The steady increase in the wear rate at higher temperatures can be attributed to the formation of transfer layer. At high temperatures transfer layers (Fig. 11) are readily formed which in turn transformed into wear particles by the action of subsequent asperities. This stain hardened transfer particles cause deep grooves on the composite surface. Thus the high temperature enhances the transfer phenomena and increases the wear rate.

D. Effects of Load

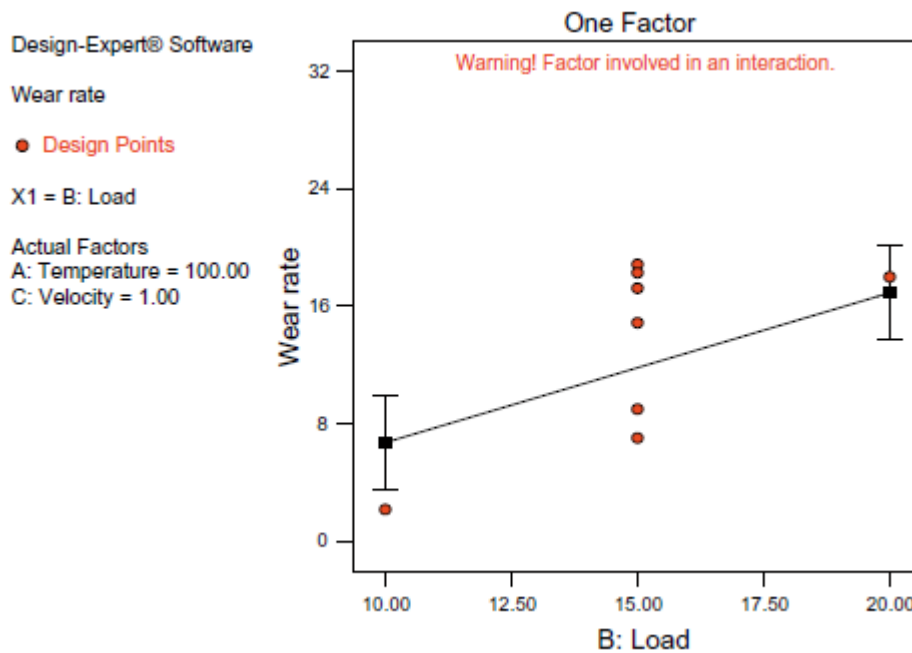


Fig. 12. Variation of wear rate with load.

Fig. 12 shows the effect of load on the wear rate. The effect of load is to increase the wear rate as it is increased. At heavy loads the SiCp loses its ability to carry the load and fractures and form debris. Also transfer layer transform into work hardened transfer particles which act as an abrasive and removes surface layer of the disc by ploughing and groove formation. The presence of fractured transfer particles are confirmed by wear debris analysis (Fig. 13). At higher temperatures it was found that effect of load was enhanced. But it is interesting to see that there was almost no interaction between load and temperature as shown by the near parallel lines in the Fig. 14.

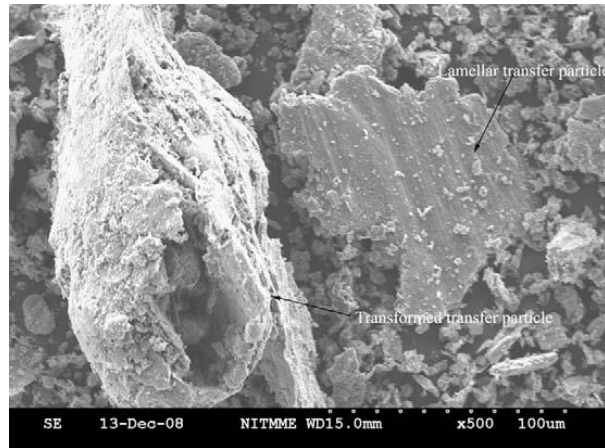


Fig. 13. Morphology of debris formed.

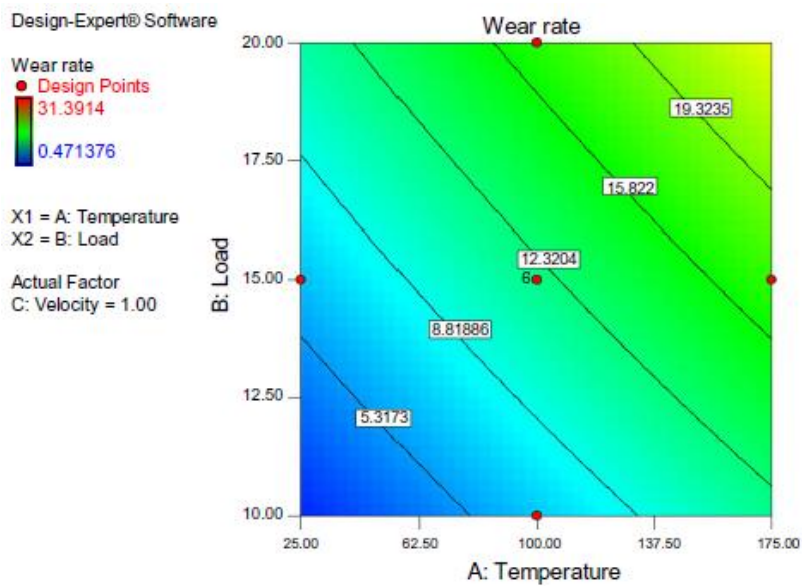


Fig. 14. Variation of wear rate with load and temperature.

E. Effects of Temperature Velocity Interaction

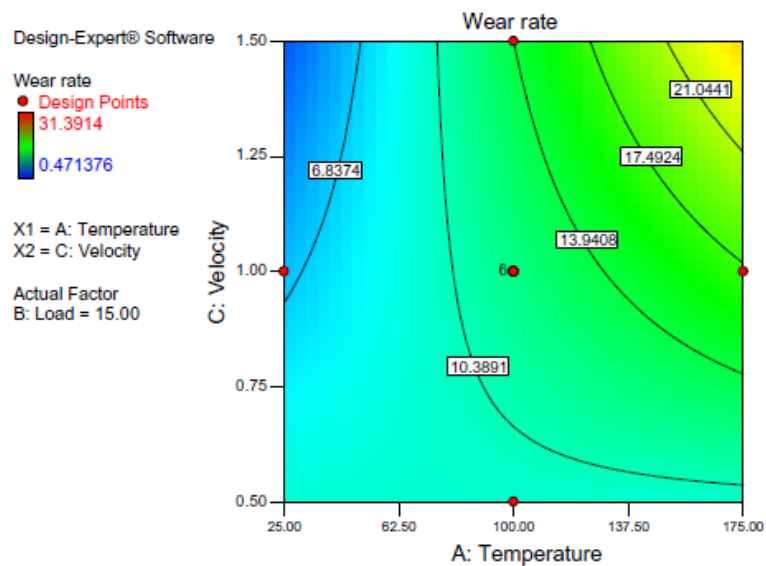


Fig. 15. Variation of wear rate with temperature and velocity.

Temperature–velocity interaction is another most influencing factor in the wear rate. The curvature of constant wear rate contours in Fig. 15 confirms the interaction of temperature and velocity. At room temperature the effect of velocity is found to be negligible but at higher temperatures the wear rate increases suddenly with increase in velocity. This can be explained by the mechanism adhesion induced tribofracture. At high temperature and velocities, the mechanism of formation of transfer layer-transformation to transfer particle-removal from the surface as debris, is quicker which caused a heavy mass loss. It can be inferred that at low velocities the oxidative mechanism is significant to diminish the effect of adhesive mechanism.

CONCLUSION

1. The order of significance of factors is: temperature > load > temperature– velocity interaction.
2. At high temperatures the wear is found to be so severe due to enhanced action of adhesion induced-tribofracture mechanism.
3. At lower loads the wear rate was found to be very less. Oxidative wear mechanism is dominant over the adhesion mechanisms resulting in a low wear rate.
4. At room temperature the effect of velocity is found to be negligible but at higher temperatures the wear rate increases suddenly with increase in velocity. This can be attributed to the significance of temperature–velocity interaction.

REFERENCES

- [1]. Surappa MK. Aluminium matrix composites: challenges and opportunities. *Sadhana* 2003;28(2):319–34.
- [2]. Thuresson Daniel. Influence of material properties on sliding contact braking applications. *Wear* 2004;257:451–60.
- [3]. Rosso M. Ceramic and metal matrix composites: routes and properties. *J Mater Process Technol* 2006;175:364–75.
- [4]. Sahin Y. Preparation and some properties of SiC particle reinforced aluminium alloy composites. *Mater Des* 2003;24:671–9.
- [5]. Sahin Y, Acilar M. Production and properties of SiCp-reinforced aluminium alloy composites. *Composites: Part A* 2003;34:709–18.
- [6]. Zhou W, Xu ZM. Casting of SiC reinforced metal matrix composites. *J Mater Process Technol* 1997;63:358–63.
- [7]. Ravikiran A, Surappa MK. Effect of sliding speed on wear behaviour of A356 Al– 30 wt.% SiCp MMC. *Wear* 1997;206:33–8.
- [8]. Mindivan Harun, Sabri Kayali E, Cimenoglu Huseyin. Tribological behavior of squeeze cast aluminum matrix composites. *Wear* 2008;265:645–54.
- [9]. Ma Tiejun, Yamaura Hideki, Koss Donald A, Voigt Robert C. Dry sliding wear behavior of cast SiC–reinforced Al MMCs. *Mater Sci Eng A* 2003;360:116–25.
- [10]. Sannino AP, Rack HJ. Dry sliding wear of discontinuously reinforced aluminium composites: review and discussion. *Wear* 1995;189:1–19.
- [11]. Sallit I, Richard C, Adam R, Robbe-Valloire F. Characterization methodology of a tribological couple: metal matrix composite/brake pads. *Mater Charact* 1998;40:169–88.
- [12]. Mosleh Mohsen, Blau Peter J, Dumitrescu Delia. Characteristics and morphology of wear particles from laboratory testing of disk brake materials. *Wear* 2004;256:1128–34.
- [13]. Blau Peter J, Meyer III Harry M. Characteristics of wear particles produced during friction tests of conventional and unconventional disc brake materials. *Wear* 2003;255:1261–9.
- [14]. Rosenberger MR, Schvezov CE, Forlerer E. Wear of different aluminum matrix composites under conditions that generate a mechanically mixed layer. *Wear* 2005;259:590–601.
- [15]. Uyyuru RK, Surappa MK, Brusethaug S. Tribological behavior of Al–Si–SiCp composites/automobile brake pad system under dry sliding conditions. *Tribol Int* 2007;40:365–73.
- [16]. Zhang Shaoyang, Wang Fuping. Comparison of friction and wear performances of brake material dry sliding against two aluminum matrix composites reinforced with different SiC particles. *J Mater Process Technol* 2007;182:122–7.
- [17]. Sahin Y. Tribological behaviour of metal matrix and its composite. *Mater Des* 2007;28:1348–52.
- [18]. Eriksson Mikael, Bergman Filip, Jacobson Staffan. On the nature of tribological contact in automotive brakes. *Wear* 2002;252:26–36.
- [19]. Eriksson Mikael, Jacobson Staffan. Tribological surfaces of organic brake pads. *Tribol Int* 2000;33:817–27.
- [20]. Chan D, Stachowiak GW. Review of automotive brake friction materials. *Proc Inst Mech Eng D: J Automobile Eng* 2004;218:953–66.
- [21]. Natarajan N, Vijayarangan S, Rajendran I. Wear behaviour of A356/25SiCp aluminium matrix composites sliding against automobile friction material. *Wear* 2006;261:812–22.
- [22]. Basavarajappa S, Chandramohan G. Wear studies on metal matrix composites: a Taguchi approach. *J Mater Sci Technol* 2005;21(6).
- [23]. Basavarajappa S, Chandramohan G, Paulo Davim J. Application of Taguchi techniques to study dry sliding wear behaviour of metal matrix composites. *Mater Des* 2007;28:1393–8.
- [24]. Sahin Y. Wear behaviour of aluminium alloy and its composites reinforced by SiC particles using statistical analysis. *Mater Des* 2003;24:95–103.
- [25]. Straffellini G, Pellizzari M, Molinari A. Influence of load and temperature on the dry sliding behaviour of Al-based metal-matrix-composites against friction material. *Wear* 2004;256:754–63.
- [26]. Stachowiak Gwidon W, Batchelor Andrew W. *Engineering Tribology*. 3rd ed. Elsevier Butterworth-Heinemann; 2005.

Biographies and Photographs:



Rahul H. Naravade, ME Design Engineering, Lecturer in Mechanical Engineering Department in P. Dr. V. V. P. Polytechnic Loni.

Prof. R. K. Belkar, ME Manufacturing, H.O.D. Mechanical Engineering Department in P. Dr. V. V. P. Polytechnic, Loni